

AUTOGENOUS SHRINKAGE OF ALKALI-ACTIVATED SLAG-FLY ASH PASTES

Zhenming LI, Marija NEDELJKOVIC, Yibing ZUO, and Guang YE

Department of Materials and Environment (Microlab), Faculty of Civil Engineering and Geosciences, Delft University of Technology, the Netherlands

z.li-2@tudelft.nl, m.nedeljkovic@tudelft.nl, y.zuo@tudelft.nl, g.ye@tudelft.nl

Introduction

Alkali-activated materials based on industrial by-products such as fly ash (FA) or blast furnace slag (BFS) have shown promising potential to replace Ordinary Portland Cement (OPC) in the construction industry¹. However, alkali-activated FA reacts slowly at room temperature and alkali-activated BFS shows quick setting and large shrinkage. When FA and BFS are blended the alkali-activated blends can counterbalance some disadvantages when FA and BFS are activated alone. It has been reported that activated BFS and FA (AASF) has high compressive strength, low porosity and good durability^{2,3}. However, the autogenous shrinkage of AASF is still higher than that of OPC⁴. The large autogenous shrinkage will hinder a wider application of this environmentally-friendly material. This paper aims to experimentally study the autogenous shrinkage phenomenon of AASF in comparison with OPC paste. The mechanism behind the autogenous shrinkage of AASF is discussed.

Materials and Method

The AASF binders were prepared with slag/fly ash ratios of 100:0, 70:30, 50:50 and 30:70 wt%, named S100, S70, S50 and S30, respectively. The chemical and mineral composition, specific gravity and particle size of the BFS and FA were shown in previous work done by Nedeljković *et al.*³. The alkaline activator consisted of sodium hydroxide and sodium silicate with modulus ratio $Ms=3.37$ (SiO_2/Na_2O , mol-based ratio). The activator to binder ratio was fixed at 0.5. The activator was prepared one day before casting. OPC paste with water-to-cement ratio of 0.3 was chosen as reference, named PC0.3. The physical and chemical parameters of the cement can be found in⁵. The pastes were mixed with a commercial Hobart mixer, with two minutes low-speed and half a minute high-speed mixing. Material storage, samples preparation and testing were performed in controlled-climate rooms at $20 \pm 1^\circ C$.

The linear autogenous shrinkage was tested using the corrugated tube method proposed by Jensen and Hansen⁶. The measurement of the autogenous shrinkage started at the final setting time (determined by Vicat needle test) of the pastes. The chemical shrinkage was tested by dilatometry method suggested by ASTM C 1608⁷. The total porosity and the pore size distribution were measured by mercury intrusion porosimetry (MIP)⁸. The internal relative humidity (RH) of the pastes as well as the RH

caused by the ions dissolved in the pore solutions was measured by Rotronic HygroLab C1 station equipped with two HC2-AW RH probes with an accuracy of $\pm 1\%$ RH.

Results and Discussion

Autogenous shrinkage and Chemical shrinkage

The evolution of autogenous shrinkage of all mixtures in the first 7 days after casting are shown in Figure 1 (the autogenous shrinkage was the mean value of three replicates). It can be clearly seen that all of the AASF mixtures underwent higher autogenous shrinkage than PC0.3. The autogenous shrinkage of S100 was around 10 times higher than that of PC0.3, reaching almost 6000 μe at the age of 7 days, while S30 shrank 3 times more than PC0.3. The autogenous shrinkage of AASF pastes increased with the slag/fly ash ratio, indicating that the incorporation of fly ash was very efficient in reducing the autogenous shrinkage of the mixtures.

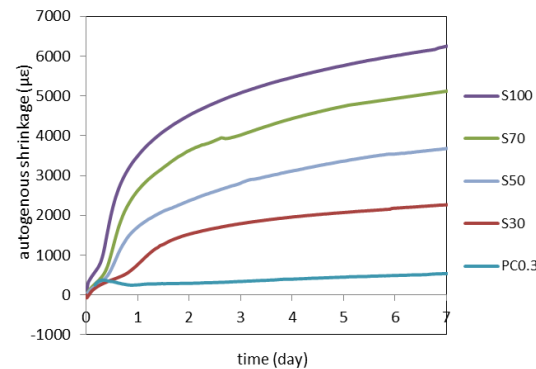


Figure 1: Autogenous shrinkage of AASF and OPC pastes

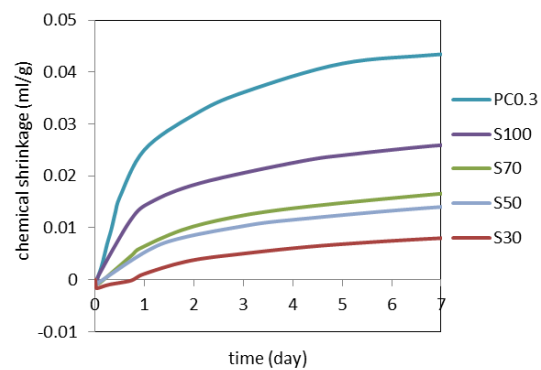


Figure 2: Chemical shrinkage of AASF and OPC pastes

In both OPC and BFS based systems, the chemical shrinkage has been considered as an important factor inducing autogenous shrinkage^{8,9}. Unlike the autogenous shrinkage, the chemical shrinkage of all AASF mixtures was lower than that of OPC (Figure 2). In ambient temperature, the reaction rate of the FA with alkali activator is much lower than that of BFS², hence it was BFS that dominated the chemical shrinkage of AASF. Therefore, it is reasonable that the chemical shrinkage of AASF pastes were lower than that of OPC, and it has been increased with the increase of BFS/FA ratio.

Pore structure

The pore structure plays a key role on the autogenous shrinkage of either OPC or alkali-activated materials^{10, 11}. As the BFS/FA ratio increased, the pore structure became denser (Figure 3). The S50, S70 and S100 pastes showed nearly no capillary pores. The finer the pore structure was, the higher capillary pressure would be induced when liquid-vapour menisci formed in the pores according to Kelvin Laplace equation^{10, 11}. Therefore, the driving force of autogenous shrinkage became higher when BFS/FA ratio was increased.

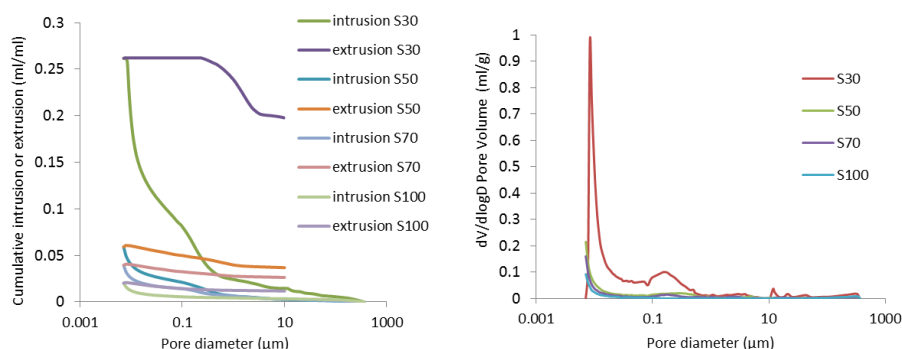


Figure 3: Pore size distribution of AASF pastes at 28 days

Internal relative humidity

The self-desiccation process has been considered as the main reason for the autogenous shrinkage of OPC^{8,10}. The internal RH is a parameter that can directly reveal the severity of the self-desiccation in the pastes. Note that in alkali-activated materials the ions dissolved in the pore solution are normally of high concentration and therefore can cause apparent RH depression of the material. After dividing the RH of the pastes by the RH of the pore solution, the RH caused only by the curvature of the menisci in AASF and OPC pastes was obtained (Figure 4).

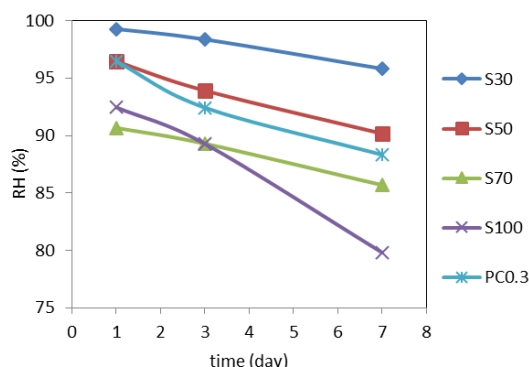


Figure 4: Internal RH of AASF and OPC pastes

S100 and S70 showed lower RH than PC0.3, and consequently suffered higher capillary pressure. The high capillary pressure was an important reason for the high autogenous shrinkage of S100 and S70. However, the RH of S50 and S30 was similar or higher than that of PC0.3, indicating that the capillary pressures existing in these two mixtures were smaller than that in PC0.3. This implies that the lower elastic stiffness of S50 and S30 may be the reason why they underwent higher autogenous shrinkage than PC0.3. In addition, Figure 4 demonstrates that the incorporation of FA raised the RH of the mixtures. This was due to the low consumption of water by the activation of FA². Therefore, the more FA in the AASF mixture, the higher internal RH the mixture would reach.

In AASF, the BFS seems to play a dominant role in autogenous shrinkage of AASF because the reaction between slag and the activator has faster reaction rate and

causes much severer self-desiccation than the reaction between FA and the activator (see Figure 2 and Figure 4). The incorporation of FA is assumed not only to relieve the self-desiccation in AASF but also to provide 'micro-aggregates' by the unreacted sphere particles, thus reducing the autogenous shrinkage of AASF. Nonetheless, the stiffness of AASF was probably reduced at the mean time when more FA was blended. More study on stiffness of AASF is needed to further explore the mechanism of autogenous shrinkage of AASF.

Conclusions

Based on the research findings in this paper, the following conclusions can be drawn:

- AASF exhibited much higher autogenous shrinkage and lower chemical shrinkage than PC0.3. The high capillary pore pressure resulting from severe self-desiccation and fine pore structure should be the main reason for high autogenous shrinkage of AASF.
- The incorporation of FA reduced the autogenous shrinkage of AASF dramatically, because of the low water consumption of the reaction between FA and activator and the 'micro-aggregates' effect provided by the unreacted sphere FA particles.

References

1. K. Arbi, M. Nedeljkovic, Y. Zuo, S. Grünwald, A. Keulen and G. Ye, "Experimental study on workability of alkali activated fly ash and slag-based geopolymer concretes", *Geopolymers route to Eliminate waste Emission Ceramics and Cement Manufacturing*, ISBN 9781326377328, 75–78 (2015).
2. K. Arbi, M. Nedeljković, Y. Zuo and G. Ye, "A Review on the Durability of Alkali-Activated Fly Ash/Slag Systems: Advances, Issues and Perspectives", *Ind Eng Chem Res*, **55** (19) 5439–5453 (2016).
3. M. Nedeljkovic, K. Arbi, Y. Zuo and G. Ye, "Physical properties and pore solution analysis of alkali activated fly ash-slag pastes", *Int RILEM Conf Mater Syst Struct Civ Eng Conf Segm Concr with Suppl. Cem Mater*, 2016.
4. N. K. Lee, J. G. Jang and H. K. Lee, "Shrinkage characteristics of alkali-activated fly ash/slag paste and mortar at early ages", *Cem Concr Compos*, **53** 239–248 (2014).
5. Z. Yu, G. Ye and X. Shen, "Delayed Ettringite Formation in Portland Cement Concrete under Moist Curing Conditions", *14th Int Congr Chem Cem*, 2015.
6. O. Mejlhede Jensen and P. Freiesleben Hansen, "A dilatometer for measuring autogenous deformation in hardening portland cement paste", *Mater Struct*, **28** (7) 406–409 (1995).
7. ASTM C 1608, "Standard test method for chemical shrinkage of hydraulic cement paste", *West Conshohocken Am Soc Test Mater*, 667–670 (2007).
8. P. Lura, *Autogenous Deformation and Internal Curing of Concrete*, 2003.
9. C. Cartwright, F. Rajabipour and A. Radli, "Shrinkage Characteristics of Alkali-Activated Slag Cements", *J Mater Civ Eng*, **27** (7) 1–9 (2014).
10. O. M. Jensen and P. F. Hansen, "Autogenous deformation and RH-change in perspective", *Cem Concr Res*, **31** (12) 1859–1865 (2001).
11. F. Collins and J. Sanjayan, "Effect of pore size distribution on drying shrinking of alkali-activated slag concrete", *Cem Concr Res*, **30** (9) 1401–1406 (2000).